Phase Transition Properties of a Ferroelectric Superlattice with Surface Modification

Hong-Li Guo[a], Xiao-Yu Kuang[a, b], Xiong Yang[a], and Rui-Peng Chai[a]

[a] Institute of Atomic and Molecular Physics, Sichuan University, Chengdu 610065, China
[b] International Centre for Materials Physics, Academia Sinica, Shenyang 110016, China

Reprint requests to X.-Y. K.; E-mail: scu_kxy@163.com

The phase diagrams of a ferroelectric superlattice with finite alternating layers are investigated by using the transverse Ising model within the mean-field approximation. The effects of surface modification are introduced through a surface exchange interaction constant and a surface transverse field parameter. The results indicate that the features of the phase diagrams can be greatly modified by changing the transverse Ising model parameters. In addition, the crossover features of the inside transverse field parameters from the ferroelectric dominant phase diagram to the paraelectric dominant phase diagram are determined for a finite alternating superlattice.

Key words: Ferroelectrics; Phase Transitions.

1. Introduction

An exciting aspect of solid-state physics is the discovery or exploration of new classes of materials. During the past decades, much effort has been devoted to the study of artificially fabricated superlattices, because the physical properties of superlattices differ dramatically from simple solids. With the advancements of experimental techniques, which make it possible to obtain well characterized samples, ferroelectric superlattices have attracted considerable attention in recent years [1 – 6]. Theoretically, the static properties including polarization, susceptibility and pyroelectricity have been studied for ferroelectric superlattices using the Ginzburg-Landau phenomenological theory [7 – 10] and the transverse Ising model (TIM) [11 – 13]. Besides, by applying the mean-field approximation, Wang et al. [14, 15] investigated extensively the ferroelectric phase transition of superlattices. Zhou and Yang [16] used the effective field theory with correlations to calculate the Curie temperature of ferroelectric superlattices formed from two alternating materials. Kaneyoshi [17] studied the phase diagrams of a transverse Ising superlattice based on the decoupling approximation in the differential operator technique. In most of the above work, surface modifications on the systems were not discussed. However, the atoms in the surface region are in an environment which is different from that of the ones in the bulk of the ferroelectric su-

perlattice, and consequently various parameters of the surface of the TIM used to describe the ferroelectric superlattice may differ from those of the bulk. In the earlier literature, Sy et al. [18, 19], have modified the surface layer to study the magnetic properties in an alternating superlattice.

In the present paper we investigate the phase transition properties of ferroelectric superlattices by modifying the transverse Ising model parameters of the surface layer. The phase diagrams are described in two ways, and the dependence of the phase diagrams on the TIM parameters is obtained by calculating the coefficient determinants.

2. Theory

We consider a finite ferroelectric superlattice with alternative slabs. A good description for H-bonded ferroelectric systems is generally believed to be the TIM within the framework of the pseudo-spin theory. The Hamiltonian of the model can be written as [14 – 19]

$$H = -\sum_i \Omega_i S_i^x - \frac{1}{2} \sum_{ij} J_{ij} S_i^z S_j^z, \tag{1}$$

where Ω_i is the transverse field, S_i^x and S_i^z are the x and z components of a spin-$\frac{1}{2}$ operator at site i, and J_{ij} is the exchange interaction constant between the i-th and j-th site, where i and j run over only the nearest-neighbouring sites. As shown in Fig. 1, we introduce
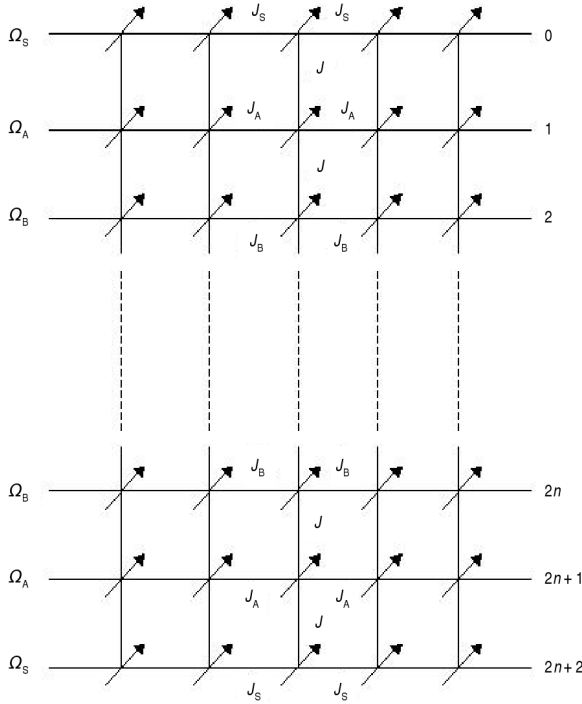
Fig. 1. Schematic illustration of a ferroelectric superlattice with the surface layer.

Ω_S, Ω_A and Ω_B to be the different transverse fields on the surface and inside alternating layers of the superlattice. We consider different exchange interaction constants, with $J_{ij} = J_S$ for the surface layers and $J_{ij} = J_A$ or $J_{ij} = J_B$ for the other alternating layers. The exchange constant between successive layers is given by $J_{ij} = J$.

By applying the mean-field approximation and assuming that the pseudo-spins in the same layer have the same values, the spin average along the z direction, $\langle S_i^z \rangle$, can be written as [14 – 19]

$$\langle S_i^z \rangle = (H_i^z / 2|H_i|) \tanh\left(|H_i| 2k_B T\right), \tag{2}$$

where

$$H_i^z = 4J_{ii}\langle S_i^z \rangle + J_{i,i+1}\langle S_{i+1}^z \rangle + J_{i,i-1}\langle S_{i-1}^z \rangle, \tag{3}$$

$$|H_i| = \sqrt{\Omega_i^2 + (H_i^z)^2}. \tag{4}$$

When the temperature approaches the Curie temperature, the spin average tends to zero. Therefore we can obtain from $(2) - (4)$ the simple expressions for the finite alternating superlattice.

For the surface layers we have

$$\begin{aligned} \tau_S S_0 &= 4J_S S_0 + J S_0, \\ \tau_S S_{2n+2} &= 4J_S S_{2n+2} + J S_{2n+2}, \end{aligned} \tag{5}$$

and for the other alternating layers

$$\begin{aligned} \tau_A S_i &= 4J_A S_i + J(S_{i+1} + S_{i-1}) \ (i = 1, 3, \cdots, 2n+1), \\ \tau_B S_i &= 4J_B S_i + J(S_{i+1} + S_{i-1}) \ (i = 2, 4, \cdots, 2n), \end{aligned} \tag{6}$$

where S_i denotes $\langle S_i^z \rangle$, and

$$\begin{aligned} \tau_S &= 2\Omega_S \coth \frac{\Omega_S}{2k_B T}, \\ \tau_A &= 2\Omega_A \coth \frac{\Omega_A}{2k_B T}, \\ \tau_B &= 2\Omega_B \coth \frac{\Omega_B}{2k_B T}. \end{aligned} \tag{7}$$

Then, the following coefficient determinant equation can be obtained:

$$\det \begin{bmatrix} X_S & -1 \\ -1 & X_A & -1 \\ & -1 & X_B & -1 \\ & & & \ddots \\ & & & -1 & X_B & -1 \\ & & & & -1 & X_A & -1 \\ & & & & & -1 & X_S \end{bmatrix}_{(2n+3)\times(2n+3)} = 0, \tag{8}$$

where $X_S = \frac{(\tau_S - 4J_S)}{J}$, $X_A = \frac{(\tau_A - 4J_A)}{J}$, and $X_B = \frac{(\tau_B - 4J_B)}{J}$. We expand the above equation as

$$\left(x_S^2 X_A / X_B\right) C_{2n+1} - 2X_S D_{2n} + C_{2n-1} = 0, \ n \geq 1, \tag{9}$$

where the two determinants D_{2n} and C_{2n-1} are defined as

$$D_{2n} = \det \begin{bmatrix} X_A & -1 \\ -1 & X_B & -1 \\ & -1 & X_A & -1 \\ & & -1 & X_B & -1 \\ & & & & \ddots \\ & & & & -1 & X_A & -1 \\ & & & & & -1 & X_B \end{bmatrix}_{2n\times 2n},$$

$$C_{2n-1} = \det \begin{bmatrix} X_B & -1 \\ -1 & X_A & -1 \\ & -1 & X_B & -1 \\ & & & \ddots \\ & & & -1 & X_A & -1 \\ & & & & -1 & X_B \end{bmatrix}_{(2n-1)\times(2n-1)}. \tag{10}$$
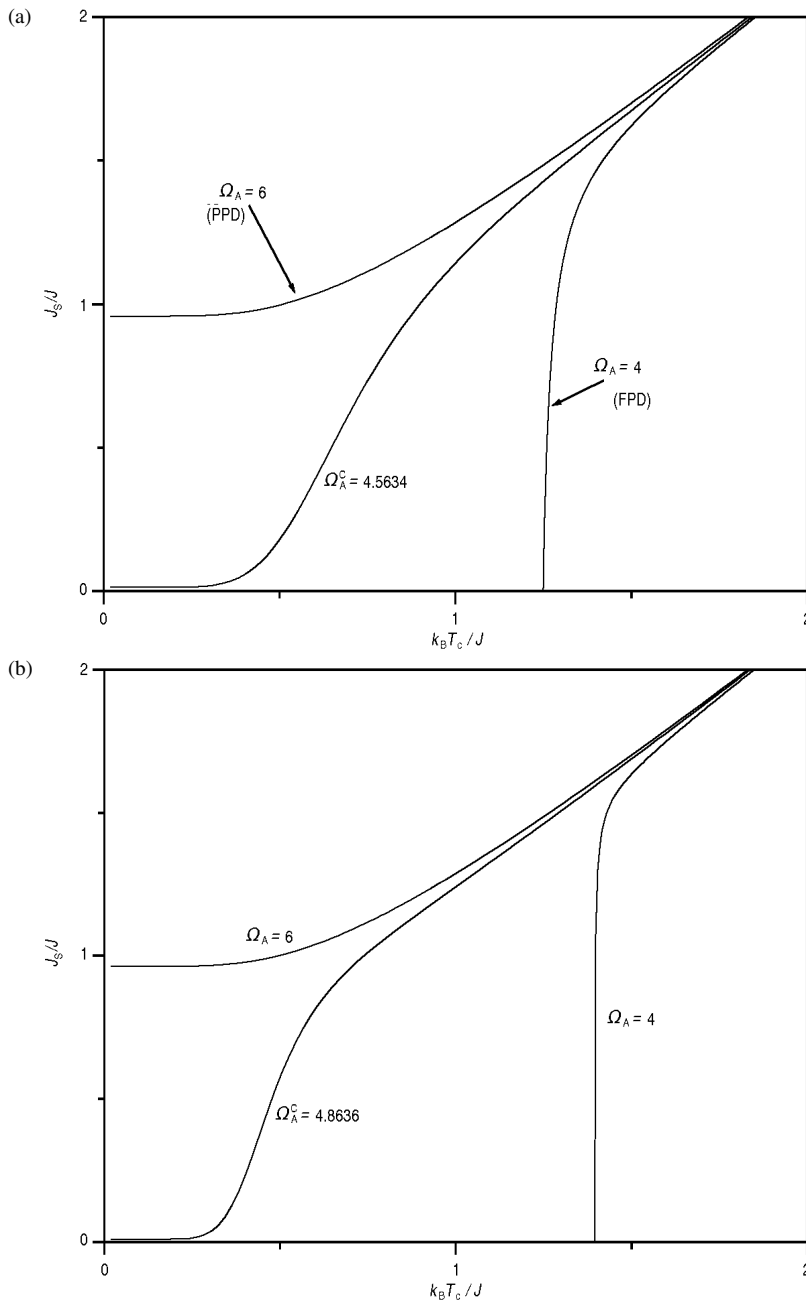
(a)

(b)

Fig. 2. The effect of Ω_A on the phase diagram ($\Omega_B > 2J_B$). All curves are for $\Omega_B/J = 3$, $J_A/J = 2$, $J_B/J = 1$, and $\Omega_S/J = 2$. (a) $n = 1$; (b) $n = 3$.

The solutions of (10) have been evaluated as [18]

$$D_{2n} = \frac{\sinh(n+1)\phi + \sinh(n\phi)}{\sinh\phi},$$

$$C_{2n-1} = \frac{2\sinh(n\phi)(\cosh\phi + 1)}{X_A \sinh\phi},$$

(11)

and here

$$2\cosh\phi = X_A X_B - 2. \tag{12}$$

3. Results and Discussion

In order to obtain a general view of the phase transition, we follow Teng and Sy's [20, 21] definitions of

(a)

(b)

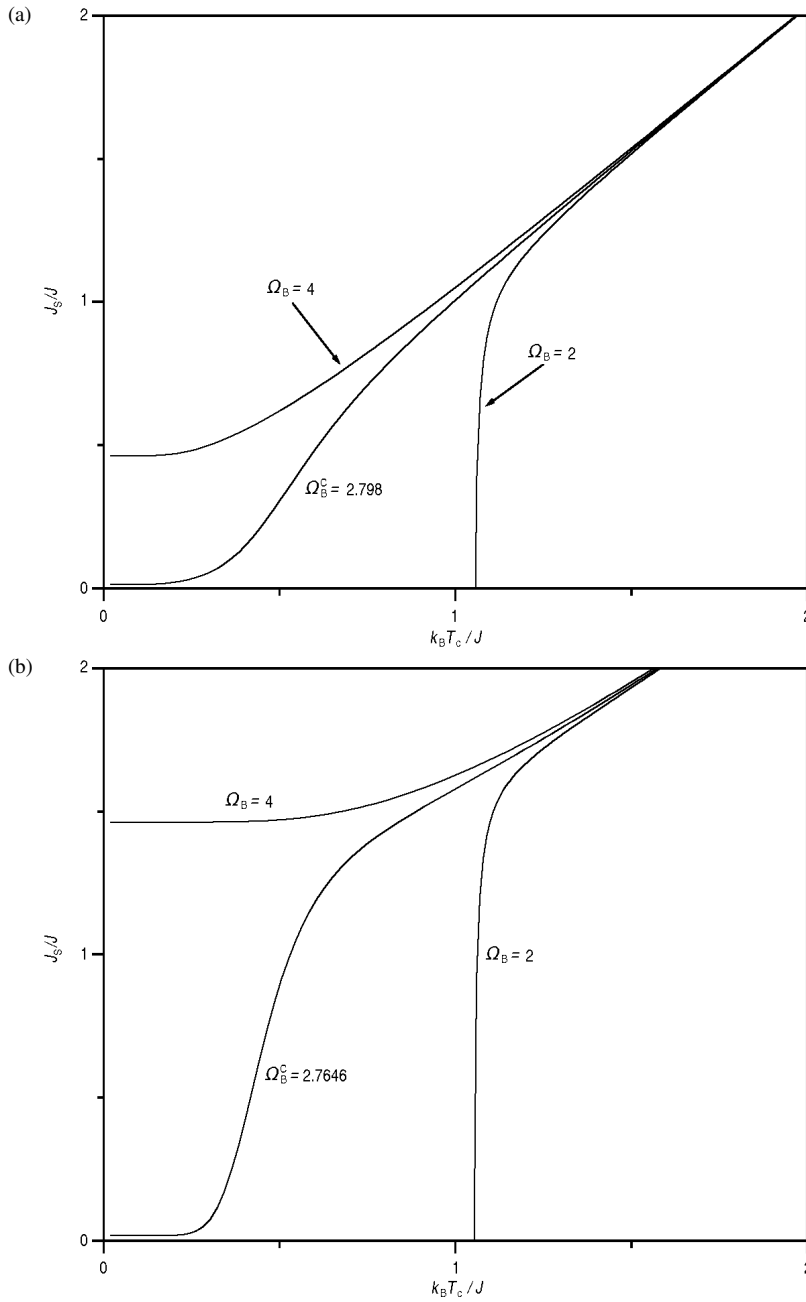Fig. 3. The effect of Ω_B on the phase diagram $(\Omega_A > 2J_A)$. All curves are for $\Omega_A/J = 5$, $J_A/J = 2$, $J_B/J = 1$, and $n = 2$. (a) $\Omega_S/J = 1$; (b) $\Omega_S/J = 3$.

the ferroelectric dominant phase diagram (FPD) and the paraelectric dominant phase diagram (PPD) (see Fig. 2a). The FPD means that, while the temperature is below a certain value, the system is ferroelectric irrespective of any J_S. This is to say, any J_S can result in a transition from a ferroelectric to a paraelectric phase with increasing the temperature. In contrast, the PPD means that, while J_S is less than a certain value, the system is paraelectric irrespective of any temperature. In other words, only larger J_S can result in a transition from a ferroelectric to a paraelectric phase with increasing the temperature [20, 21].

In most of the discussions of ferroelectric thin films, the phase diagrams are described in two ways: the re-
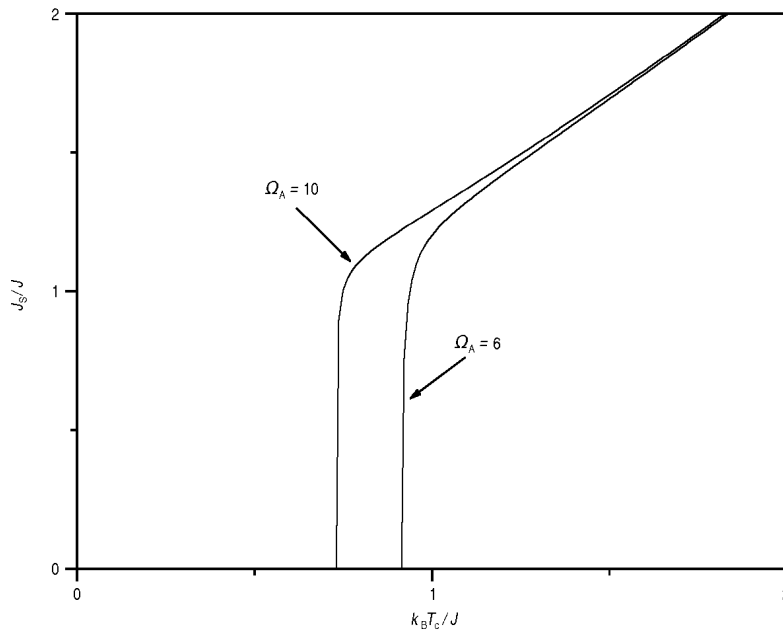
Fig. 4. The effect of Ω_A on the phase diagram ($\Omega_B < 2J_B$). All curves are for $\Omega_B/J = 1.8$, $J_A/J = 2$, $J_B/J = 1$, $\Omega_S/J = 2$, and $n = 2$.
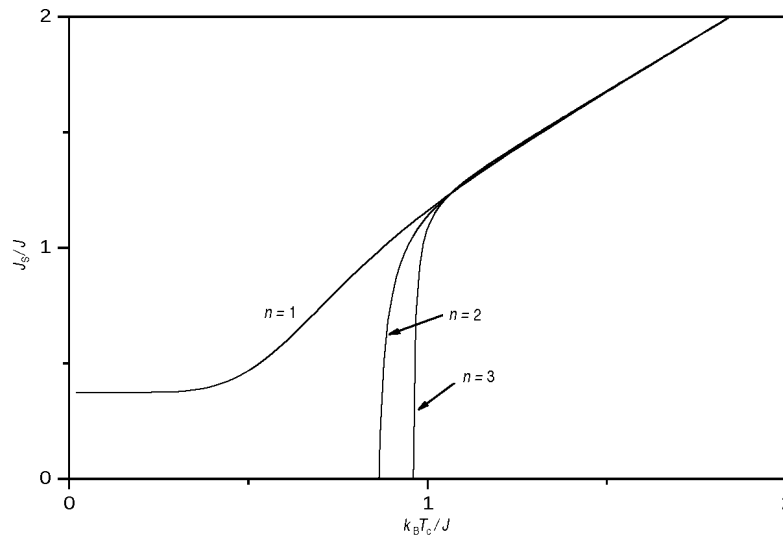

Fig. 5. The effect of the layer number n on the phase diagram. All curves are for $\Omega_A/J = 4.6$, $\Omega_B/J = 3$, $J_A/J = 2$, $J_B/J = 1$, and $\Omega_S/J = 2$.

lations between the Curie temperature, T_c, and the surface exchange interaction, J_S [18–23], as well as the Curie temperature and the surface transverse field, Ω_S [23–25]. In this paper we will discuss the effects of the TIM parameters on the phase diagrams for a finite alternating superlattice, with use of the definitions of the FPD and PPD. The numerical calculations for the two different sorts of phase diagrams in the TIM are given in the figures.

Figures 2, 3, 4 and 5 give the phase diagrams between the Curie temperature and the exchange interac-

tion on the surface. Figures 2 and 3 give the curves of different values of the transverse field Ω_A or Ω_B, and it is shown that the phase diagram depends sensitively on Ω_A or Ω_B. The larger the transverse field Ω_A or Ω_B, the larger is the range of the paraelectric phase; and the smaller the parameter Ω_A or Ω_B, the larger is the range of the ferroelectric phase. The crossover feature from the FPD to PPD is also shown in Figure 2. It is obvious that, when Ω_A or Ω_B have less than the crossover value Ω_A^C or Ω_B^C, the phase diagram is in the FPD, and any J_S can result in a transition from the ferroelectric
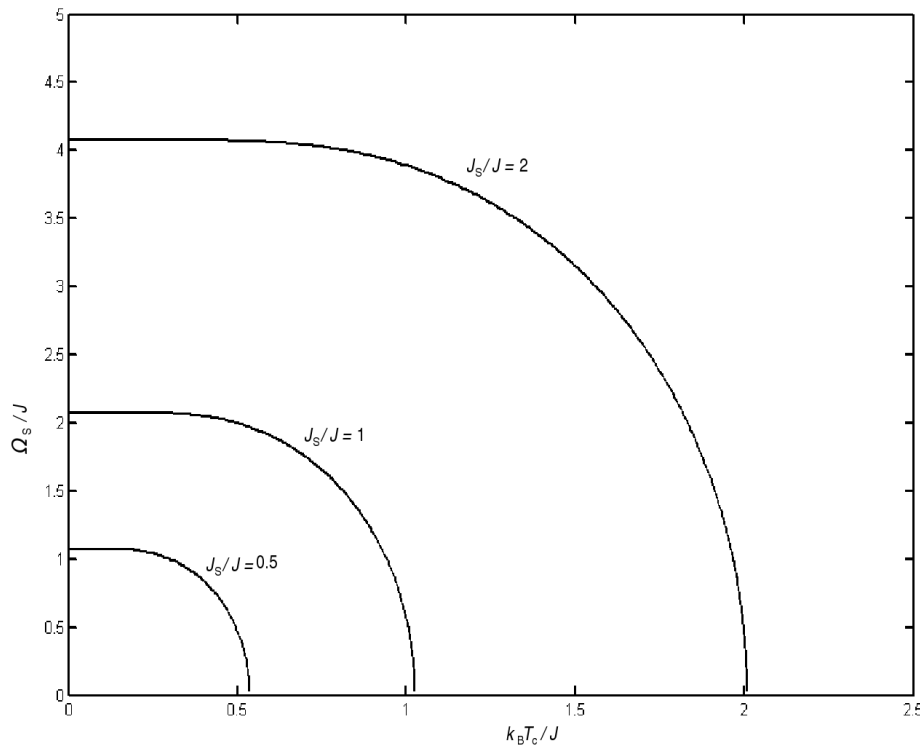
Fig. 6. The effect of J_S on the phase diagram. All curves are for $\Omega_A/J = 6$, $\Omega_B/J = 3$, $J_A/J = 2$, $J_B/J = 1$, and $n = 2$.

to the paraelectric phase with increasing the temperature. However, when Ω_A or Ω_B is larger than Ω_A^C or Ω_B^C, the phase diagram is in the PPD, and only larger J_S can result in a transition from the ferroelectric to the paraelectric phase with increasing the temperature. Figures 2a and 2b also reveal the effect of the layer number on the crossover value of the parameter Ω_A. The thicker the superlattice, the larger is the crossover value Ω_A^C. Figures 3a and 3b also show the effect of the surface transverse field Ω_S on the crossover value of the parameter Ω_B. The larger the surface transverse field Ω_S, the smaller is the crossover value Ω_B^C. Simultaneously, we find that larger Ω_S will result in a larger range for the paraelectric state as well. In addition, the dependence of Ω_A on Ω_S is similar to that of Ω_B, and the dependence of Ω_B on the superlattice thickness is also similar to that of Ω_A; so we do not give a detailed discussion of these situations.

However, comparing Fig. 2 and Fig. 4, we find that the appearance of the crossover value of the parameter Ω_A is determined by the relation between the transverse field Ω_B and the exchange interaction J_B. Figures 2a and 2b indicate that, when $\Omega_B > 2J_B$, there exists a crossover value Ω_A^C from the FPD to PPD. Figure 4 shows that, when $\Omega_B < 2J_B$, the phase diagram

is always in the FPD, irrespective of Ω_A, and this is to say, there does not exist a crossover value Ω_A^C. At the same time, it can be seen from Fig. 3 that in the region of $\Omega_A > 2J_A$ there always exists a crossover value Ω_B^C in the phase diagram. In fact, the numerical calculations reveal that in the region of $\Omega_A < 2J_A$, there does not exist a crossover value Ω_B^C. These phase transition properties are similar to those of ferroelectric thin films [20, 23].

Figure 5 shows the dependence of the phase diagram on the thickness of the superlattice. It can be clearly seen that the five-layer superlattice has no phase transition, and it is always paraelectric in the entire temperature range, but only if the surface interaction strength J_S is sufficiently weak. When the ferroelectric superlattice is thicker than five layers, the more layers the superlattice contains, the larger is the range of the ferroelectric phase.

Figures 6 and 7 are the phase diagrams showing the relations between the Curie temperature and the transverse field on the surface. Figure 6 shows the dependence of the phase diagram on the surface exchange interaction J_S; it can be seen that a larger J_S/J will result in a larger range for the ferroelectric state. Figure 7 shows how the phase diagram depends on the exchange
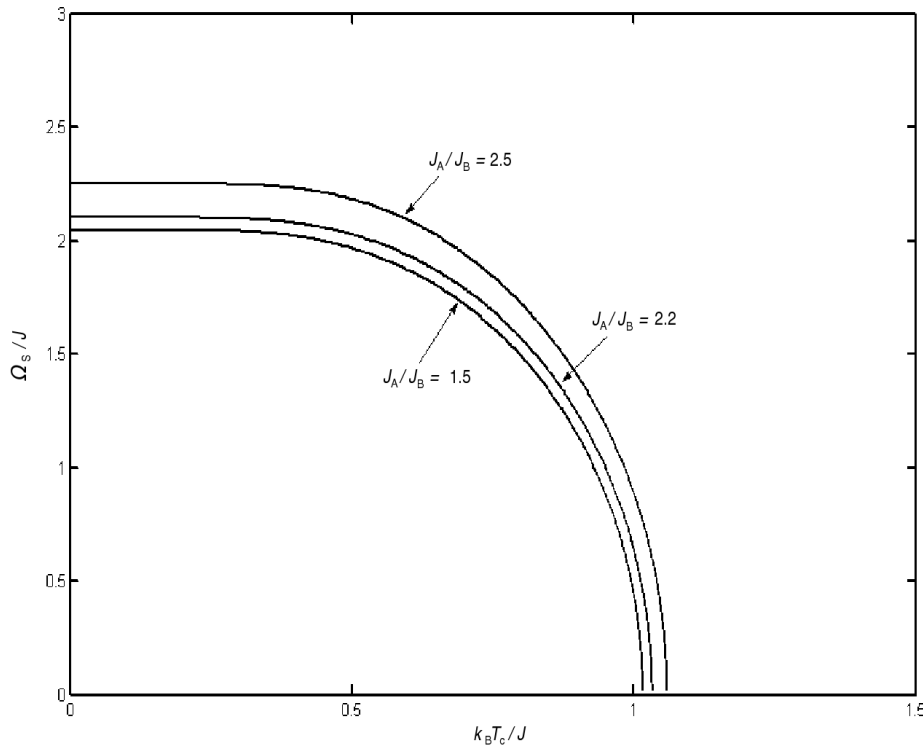
Fig. 7. The effect of J_A/J_B on the phase diagram. All curves are for $\Omega_A/J = 6$, $\Omega_B/J = 3$, $J_B/J = 1$, $J_S/J = 1$, and $n = 2$.

interaction constants J_A and J_B. One sees from Fig. 6 that the larger the ratio J_A/J_B, the larger is the ferroelectric range in the phase diagram. Obviously, the phase diagram depends sensitively on the exchange interaction J_S, J_A and J_B.

4. Conclusion

In summary, we have studied the ferroelectric phase properties of a finite alternating superlattice described by the transverse Ising model. Although the mean-field approximation, compared with the effective field theory and the decoupling approximation in the differential operator technique, may exaggerate the ferroelectric feature of a superlattice, our numerical results can reveal explicitly how the phase diagram depends on the transverse Ising model parameters by using the mean-field approximation. Meanwhile, the crossover features

of the parameters from the FPD to PPD are given for the ferroelectric superlattice. In fact, the surface modification may be similarly introduced into other transverse Ising superlattices for studying the ferroelectric phase transitions. We hope that these results may provide some useful information for theoretical and experimental work on ferroelectric superlattices, with the developments of the experimental techniques in this field.

[1] K. Iijima, T. Terashima, Y. Bando, K. Kamigaki, and H. Terauchi, Jpn. J. Appl. Phys. **72**, 2840 (1992).
[2] T. Tsurumi, T. Suzuki, M. Yamane, and M. Daimon, Jpn. J. Appl. Phys. **33**, 5192 (1992).
[3] A. Erbil, Y. Kim, and R. A. Gerhardt, Phys. Rev. Lett. **77**, 1628 (1996).
[4] H. Tabata and T. Kawai, Appl. Phys. Lett. **70**, 20 (1997).
[5] B. D. Qu, M. Evstigneev, D. J. Johnson, and R. H. Prince, Appl. Phys. Lett. **72**, 1394 (1998).
[6] I. Kanno, S. Hayashi, R. Takayama, and T. Hirao, Appl. Phys. Lett. **68**, 382 (1996).

[7] D. R. Tilley, Solid State Commun. **65**, 657 (1988).

[8] D. Schwenk, F. Fishman, and F. Schwabl, Phys. Rev. B **38**, 11618 (1988).

[9] D. Schwenk, F. Fishman, and F. Schwabl, J. Phys. Condens.: Matter **2**, 5409 (1990).

[10] D. Schwenk, F. Fishman, and F. Schwabl, Ferroelectrics **104**, 349 (1990).

[11] B. D. Qu, W. L. Zhong, and P. L. Zhang, Phys. Lett. A **189**, 419 (1994).

[12] B. D. Qu, W. L. Zhong, and P. L. Zhang, Jpn. J. Appl. Phys. **34**, 4114 (1995).

[13] C. L. Wang and S. R. P. Smith, J. Korean Phys. Soc. **32**, 382 (1998).

[14] C. L. Wang, Y. Xin, X. S. Wang, W. L. Zhong, and P. L. Zhang, Phys. Lett. A **268**, 117 (2000).

[15] X. S. Wang, C. L. Wang, and W. L. Zhong, Solid State Commun. **122**, 311 (2002).

[16] J. H. Zhou and C. Z. Yang, Solid State Commun. **101**, 639 (1997).

[17] T. Kaneyoshi, Physica A **291**, 387 (2001).

[18] H. K. Sy, J. Phys.: Condens. Matter **4**, 5891 (1992).

[19] H. K. Sy, Phys. Rev. B **45**, 4454 (1992).

[20] B. H. Teng and H. K. Sy, Physica B **348**, 485 (2004).

[21] B. H. Teng and H. K. Sy, Phys. Rev. B **69**, 104115 (2004).

[22] C. L. Wang, W. L. Zhong, and P. L. Zhang, J. Phys.: Condens. Matter **3**, 4743 (1992).

[23] X. Yang, X. Y. Kuang, and Ch. Lu, Solid State Commun. **139**, 397 (2006).

[24] T. Kaneyoshi, Physica A **293**, 200 (2001).

[25] T. Kaneyoshi, Physica A **319**, 355 (2003).